Chapter 7
Radical transfer in DNA photolyase

7.1. Introduction

The reactive environment of the cells, the presence of a variety of toxic substances and the exposure to UV light or ionizing radiation cause changes and damages in the structure of DNA, as for instance excision or modification of bases or alternation of sugar-phosphate groups. Some of these reactions occur relatively often and with high rates. To maintain genetic stability, cells protect themselves against these types of damages. Such repair is possible since DNA contains and keeps its information in double helical structure. There are several pathways to repair different types of DNA damages. Even very simple organisms as *Escherichia coli* possess such enzymes and pathways. In fact, the main DNA repair processes in *E. coli* and mammalian cells are chemically quite similar. Here, will be explain one of the most frequent damages – pyrimidine dimers and the function of DNA photolyase enzyme which repairs these DNA defects.

7.1.1. Splitting the pirymidine dimer by photolyase

Far-UV light (200-300 nm) is harmful to the biological function of DNA. Its action results in the formation of a cyclobutyl ring between adjacent thymine residues on the same DNA strand yielding an intrastrand thymine dimer. Similar cytosine and thymine-cytosine dimers can be formed but at lesser rates. Such pyrimidine dimers locally distort the DNA base pair structure so that it can form neither a proper transcriptional nor replicational template, what leads to cytotoxic and mutagenic effects (Harm, 1980).

DNA photolyase is an enzyme that catalyzes the repair of major ultraviolet-induced DNA lesions, cyclobutane pyrimidine dimers or (6-4)-photoproducts, using the energy of near-ultraviolet and visible light (300-500 nm) (Kim & Sancar, 1993; Sancar, 1994, 1996). This enzyme is widespread in nature, ranging from bacteria to multicellular eukaryotes. It is a monomeric protein with a relative molecular mass between 55 kD to 65 kD. A polypeptide chain from *E. coli*, for example, consists of 471 residues, while the polypeptide chain from *A. nidulans* has 483 residues. DNA photolyase contains two non-covalently bound cofactors – one flavin adenine dinucleotide (FAD), and as second cofactor the chromophore 5,10-methenyltetrahydrofolate (shortly folic acid, MTHF) or alternatively 8-hydroxy-5-deazaflavin (HDF) molecule. On the basis of the chromophore, photolyases are divided into two classes. The folate class of photolyases is characterized by the MTHF cofactor as in *E. coli*, while HDF is present in the deazaflavin class as for instance in *A. nidulans*. These cofactors are at the same time the photoactive components of this enzyme. The function of the second cofactor is to absorb 300- to 500-nm light and to transfer the excitation energy to the non-covalently bound $FADH^-$, which in turn transfers an electron to the pyrimidine dimer, thereby splitting it (see Figure 7.1, bottom part). Finally, the resulting pyrimidine anion reduces the $FADH^\bullet$ and the repaired DNA is released. Inspection of the crystal structure of photolyase

reveals a U-shaped $FADH^-$, located in a cavity that may act as the active site accessible for docking with the pyrimidine dimer (Hahn et al., 1998).

Hence, the enzyme photolyase repairs UV induced damage in DNA by splitting the ring of the predominant photoproduct, the cis,syn-cyclobutane pyrimidine dimer, into the corresponding pyrimidine monomers. Current data support the following major steps in the photorepair mechanism: (i) recognition of the DNA defect by photolyase and its structure-specific binding to the dimer in a light-independent event (Sancar et al., 1985; Sancar & Sancar, 1988; Kim & Sancar, 1991), (ii) excitation of the photoactive cofactor $FADH^-$, either directly or via excitation energy transfer from MTHF (Payne et al., 1987), (iii) electron transfer from the excited $FADH^-$ to the pyrimidine dimer (Kim et al., 1993), (iv) splitting of the cyclobutane ring and back electron transfer to $FADH^\bullet$ (Kim & Sancar, 1993) and finally, (v) desorption of the enzyme from the repaired DNA substrate. Some variations in the mechanism of splitting the dimer were experimentally also observed. It is known that W277 can absorb a 280-nm photon and thereby split the dimer by a direct ET reaction (Kim et al., 1992).

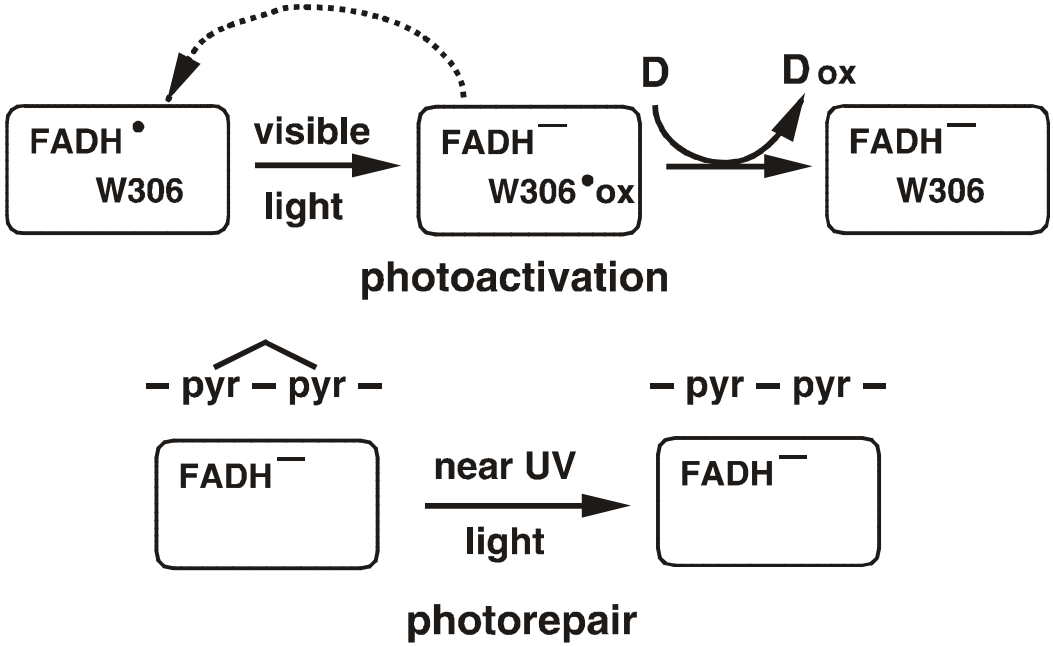

Figure 7.1: Schematic representation of two main processes in DNA photolyase – photoactivation shown on the top part and photorepair shown on the bottom part of the figure. (D is an exogenous electron donor; pyr is pyrimidine base in DNA). See text for details.

The flavin adenine dinucleotide (FAD) molecule is the essential catalytic cofactor of this enzyme. It functions only when the FAD is fully reduced ($FADH^-$). In isolated DNA photolyase, FAD is typically in the inactive semireduced state ($FADH^\bullet$), but it can be easily reduced to the catalytically active $FADH^-$ state by illumination with visible or near-UV light in the presence of an exogenous electron donor, in a process called photoactivation (see Figure 7.1, top part). Since, in the present application we were interested only to examine the energetics of the photoactivation process, some more details and experimental results will be provided in the next section.

7.1.2. Mechanism of photoactivation

In the resting state of the DNA photolyase from *E. coli* (Figure 7.2), flavin is in the neutral radical form $FADH^{\bullet}$, which is catalytically inert. UV/VIS irradiation converts the flavin to the reduced form $FADH^{-}$. Namely, the MTHF cofactor absorbs a blue light photon (~510 nm) (Kim et al., 1993) and then within 200 ps excites flavin of FAD by an energy transfer with 60% efficiency (Tamada et al., 1997). The excited $FADH^{\bullet}$* state is reduced to the catalytic active $FADH^{-}$ form by the ET, resulting in a positively charged tryptophan W306 (Kim et al., 1991), which is located on the protein surface about 13.4 Å away from the flavin. The solvent accessible W306 remains in the radical state (Kim et al., 1993) with a life time of about 10 ms limited by back transfer (Heelis et al., 1990; Li et al., 1991). Thus, it stabilizes the active state of the anionic flavin $FADH^{-}$. In photolyase from *A. nidulans*, the radical state resides on a tyrosine (Aubert et al., 1999a, 1999b).

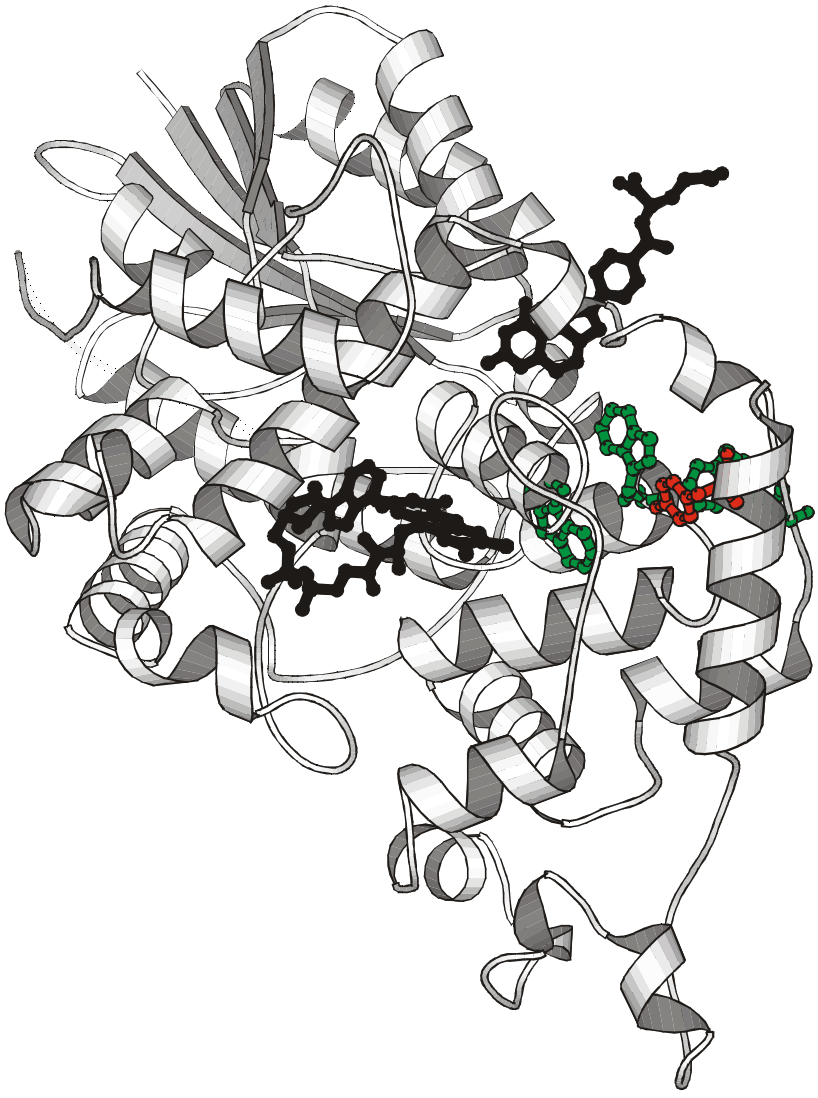

Figure 7.2: X-ray structure of DNA photolyase from *E. coli* (PDB code, 1DNP; Park, et al., 1995). The cofactors and at the same time the photoactive components of this enzyme are the flavin adenine dinucleotide (in the active state $FADH^{-}$), and 5,10-methenyltetrahydrofolate (MTHF), shown in black color, in the middle and on the top of the structure, respectively. The three tryptophans from the triad (from left to right W382, W359 and W306) are shown in green. The tyrosine Y464 is displayed in red color.

The role of amino acid radicals as intermediates in ET and hydrogen atom transfer is a topic of growing interest and research activity in enzymatic reactions (Sigel & Sigel, 1994; Stubbe & van der Donk, 1998). The most known examples for transfer of radical character within a protein, can be found in ribonucleotide reductase (tyrosinyl radical; Reichard & Ehrenberg, 1983; Graeslund & Sahlin, 1996), photosynthetic water-oxidizing enzyme (tyrosine Y_Z; Barry & Babcock, 1987; Hoganson & Babcock, 1997), and photolyase (tryptophanyl radical; Heelis et al., 1990; Kim et al., 1993). In class I ribonucleotide reductase, radical transfer occurs from a tyrosyl radical to a cysteine over a distance as large as 35 Å (Uhlin & Eklund, 1994, Sjoberg, 1994). It is currently debated whether this kind of long-range radical transfer occurs by electron transfer, followed by proton release, or by H-atom transfer, that is a simultaneous transfer of an electron and proton. In the low dielectric medium of a protein, a hydrogen transfer mechanism can be advantageous, since one saves the energy required for charge separation. Therefore, in RNR this radical transport mechanism is under discussion (Siegbahn et al., 1997; Page et al., 1999). In photolyase, the ET process is photo-activated. Therefore, there is enough energy available to initialize the charge separation process. However, also here the transfer of a neutral hydrogen may have some advantage, since it would not require a charge reorganization energy as is needed for an ET. Although in the low dielectric medium of a protein the reorganization energy for an ET is small and the energy barriers that a transferred hydrogen has to overcome may be large.

The mechanism of photo-activation was recently studied for *E. coli* photolyase at pH=7.4 by time resolved absorption spectroscopy after selective excitation of $FADH^{\bullet}$ in the pico- to millisecond time regime (Aubert et al., 2000). To establish whether $W^{\bullet}$ is formed by hydrogen atom transfer or by electron transfer and subsequent deprotonation, the kinetics of flash-induced absorbance changes in the nanosecond timescale was measured. A bleaching with a time constant of 300 ns was observed at all wavelengths from the 300-645 nm range where deprotonation of $WH^{\bullet+}$ (H refers to the N1 proton of the indole ring) gives characteristic absorbance changes. The spectrum changes clearly indicating that the 300-ns phase corresponds to the deprotonation of $WH^{\bullet+}$, and that the radical mechanism of photolyase functions via electron transfer, followed by $WH^{\bullet+}$ deprotonation.

After illumination with UV/VIS light (630 nm), it was found that the excited $FADH^{\bullet}$* state decays in 30 ps before the formation of a $WH^{\bullet+}$ species (Aubert et al., 2000). The solvent accessible tryptophan residue W306 is as far as 13.4 Å (shortest edge-to-edge distance) from flavin, what excludes a direct or superexchange-mediated electron transfer from W306 to $FADH^{\bullet}$*. However, two other tryptophan residues, W382 and W359, are located in between (see Fig. 7.3), suggesting an electron transfer in three steps. The results of theoretical calculations using the method of atomic tunneling currents (Cheung et al., 1999) also support the crucial role of the tryptophan triad in the ET pathway of *E. coli* photolyase. Presumably, the electron is first transferred from the nearest tryptophan W382 to flavin in about 30 ps. Then, the electron is transferred along the triad W382–W359–W306 generating the cationic radical $WH^{\bullet+}306$ in less than 10 ns, a time that is instrument limited (Aubert et al., 2000). The cationic radical $WH^{\bullet+}306$ deprotonates to the neutral radical $W^{\bullet}306$ with a time constant of 300 ns. With an estimation that W306 behaves as in solution (pK_a=4 for $WH^{\bullet+}$; Tommos et al. 1999), it would give a decrease in free energy of about 200 meV at pH=7.4 (Aubert et al., 2000). This energy decrease is essential to prevent a fast charge recombination and stabilizes the $FADH^{-}$ state. Finally, the radical $W^{\bullet}306$ relaxes exponentially with a time constant of 17 ms due to charge recombination. The recombination kinetics is strongly accelerated at lower pH. Thus, the time constant of recombination is 17 ms at pH 7.4, 7 ms at pH 6.5 and even 0.9 ms at pH 5.4. Hence, $W^{\bullet}306$ needs to be protonated before recombination. The acceleration of the recombination with decreasing pH indicates that this is actually the recombination

pathway. A radical transfer to the closest tyrosine Y464 (Fig. 7.3), 3.6 Å away from the W306, was not observed, in contrast to the photolyase from *A. nidulans*, where the electron transfer between tyrosine and tryptophan was detected. Hence, the final radical state resides on a tyrosinyl radical (Aubert et al., 1999a and 1999b), but it is still unknown which tryptophan and tyrosine residues participate in the radical transfer chain there.

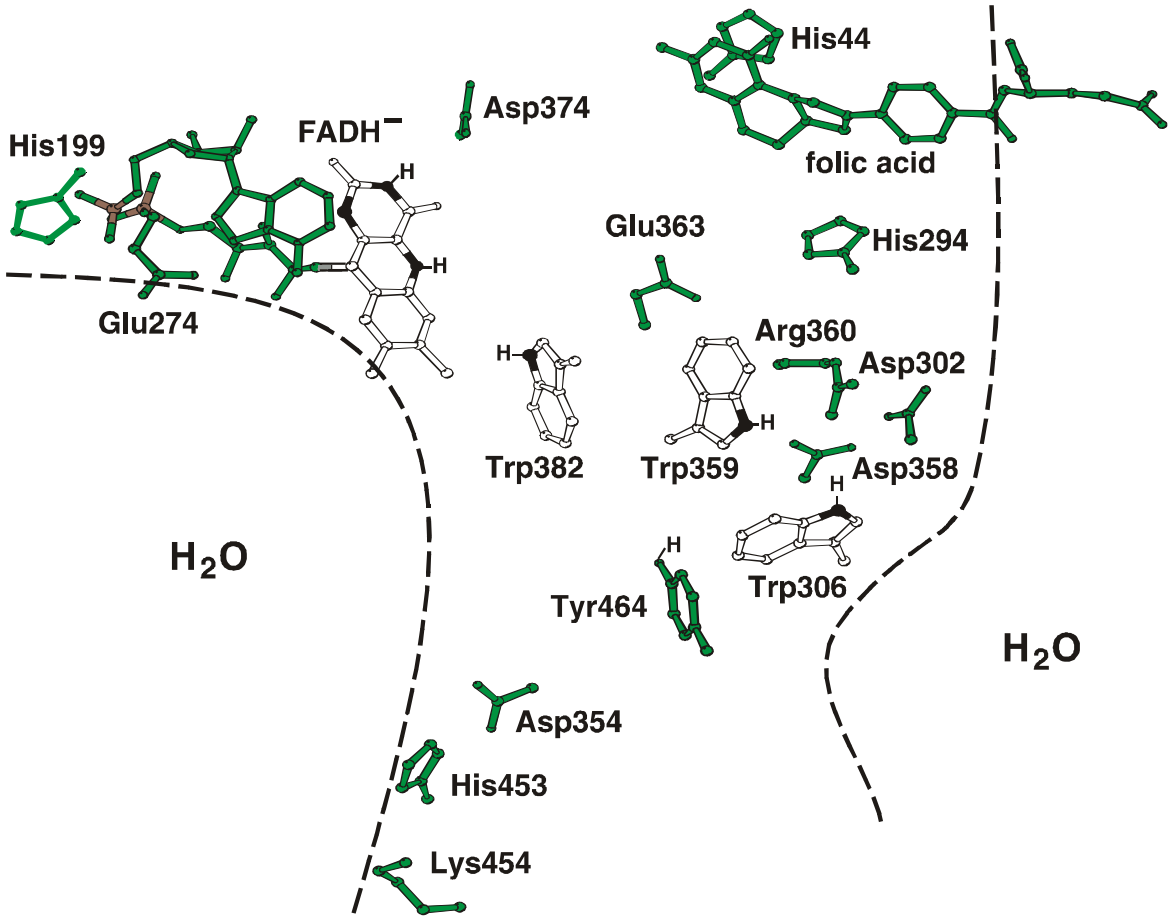

Figure 7.3: Structure of the cofactors FADH, folic acid, the tryptophan triad W382—W359—W306 in DNA photolyase. The solvent boundary of photolyase is displayed by a dashed line. The hydrogen atoms relevant for deprotonation of the tryptophans and Tyr464 are explicitly indicated. Titratable residues that are close to the tryptophan triad and vary their protonation state with a change in the charge state of the tryptophans are also shown.

With respect to the deprotonation of the tryptophanyl radical it is important to identify the proton acceptor. Increasing glycerol concentration in the solvent causes a pronounced decrease in the rate of $WH^{\bullet+}$ deprotonation, suggesting that the proton from $WH^{\bullet+}$ is released to the solvent rather than being transferred to some other proton acceptor residue in the protein. The solvent contains two potential proton acceptors in sufficient concentration – buffer and H_2O molecules. Increasing concentration of Tris buffer accelerates the deprotonation of $WH^{\bullet+}$, and this acceleration is much more pronounce at high pH. It shows that the unprotonated Tris buffer molecules are the dominating proton acceptors at high concentration of Tris buffer. The deprotonation rate constant for $WH^{\bullet+}306$ of about $5.3x10^6$

s^{-1} (Aubert et al., 2000) was estimated by extrapolation Tris buffer concentration to zero. That value is attributed to a direct proton transfer from $WH^{\bullet+}$ to H_2O molecules of the solvent. Hence, the conclusion is that the solvent molecules are the dominating proton acceptors for deprotonation of tryptophanyl cation radical.

The X-ray structure of *E. coli* photolyase (Park et al., 1995) reveals important differences between the environments of the three tryptophans. The indole ring of W306 is partially surrounded by polar amino acids. Its ring nitrogen is directly exposed to a shallow pocket that is open to the solvent and that can accommodate a water molecule. This situation should favor proton transfer from the $WH^{\bullet+}306$ cation radical to the solvent. In contrast, W382 is buried in the hydrophobic interior of the protein. There is no potential proton acceptor within 5 Å around its ring nitrogen, what excludes an efficient deprotonation of the $WH^{\bullet+}382$ cation radical. The indol ring of W359 is surrounded by both hydrophobic and polar amino acids. The ring nitrogen is hydrogen bonded to a more buried water molecule that might assist deprotonation of the $WH^{\bullet+}359$ cation radical. However, experimental data with time resolution of 10 ns (Aubert et al., 2000), together with data on the W306F mutant (Li et al., 1991), do not give any indication for a deprotonation of the $WH^{\bullet+}359$ cation radical.

The different polarities of the tryptophan environments should be also relevant for the energetics of the electron transfer reaction. Generally, the redox potential of the $WH^{\bullet+}/WH$ pair is higher in a hydrophobic protein environment than in aqueous solution (Tommos et al., 1999), since the positively charged tryptophanyl radical (oxidized form) can be accommodated better in a medium of higher dielectric constant than in low dielectric protein. Therefore, it is likely to be some decrease of the free energy of the $WH^{\bullet+}$ states in the order W382, W359, W306, favoring radical localization on W306 already, before its deprotonation.

The aim of our electrostatic computations is to support and complete the model of radical transfer and stabilization of the catalytically active $FADH^-$ state by calculating the energetics of the redox and protonation reactions in DNA photolyase. For this purpose, we evaluated the redox potentials and electrostatic energies of all states that are potentially relevant for radical transfer during photoactivation of DNA photolyase from *E. coli*, by solving the linear Poisson-Boltzmann equation and calculating the Boltzmann weighted probabilities for the different charge states of FAD and the tryptophan triad. A similar approach was recently applied on the bacterial photosynthetic reaction center (Rabenstein et al., 1998a, b; 2000) studing the ET between two quinones that is simultaneously coupled with proton uptake.

7.2. Methods

7.2.1. Calculations of protonation and redox patterns

In our calculations, we used the crystal structure of the DNA photolyase from *Escherichia coli* (PDB code, 1DNP) with a resolution of 2.3 Å, solved by Park, et al., 1995. The PDB-entry for the *E. coli* photolyase structure contains two sequentially identical subunits (chain *A* and *B*) that differ in the positions of the crystal water molecules. Moreover, the RMS deviations between two chains are very small (0.33Å for all heavy atoms and 0.03Å for residues in the catalitical core). The RMSD show that the two chains differ only in the position of a few residues on the protein surface. Since we did not consider water molecules

explicitly, we used only chain *A* for our computations. DNA photolyase from *Escherichia coli* possesses 471 residues and two cofactors – one flavin adenin dinucleotide (FAD) and one folic acid (MTHF). Atomic coordinates of the two last residues at the C-terminus (Gly 470 and Lys 471) are not available from the X-ray structure, because they are disordered. Since these residues are far away from the flavin of FAD and the active site of the protein, which contains the tryptophan triad, we ignored and did not model them additionally.

All 372 crystallographic water molecules were removed, since the position of their hydrogen atoms are not known. The influence of water was considered exclusively by a high dielectric continuum ($\varepsilon = 80$) outside the protein and in cavities that were formed by their removal. In some of the recent applications, selected water molecules were explicitly included in pK_a calculations (Cometta-Morini et al., 1993; Sampogna & Honig, 1994; Gibas & Subramaniam, 1996; Ullmann et al., 1996). Different selection schemes for the water molecules were used and they gave results, which differed from those obtained without explicit water molecules. In principle, one can use all or only a few selected crystal water molecules or even additional solvent molecules can be included. But generally, the agreement between calculated and measured pK_a values is better without explicit water molecules (as was shown for hen egg lysozyme by Gibas & Subramaniam, 1996). The reason for that is the unknown orientation of water hydrogens, that is essential for these calculations.

We used an all atom representation of DNA photolyase, where all hydrogens were treated explicitly. Chain *A* contains 3855 non-hydrogen heavy atoms. The coordinates of hydrogen atoms were generated with the HBUILD command of CHARMM22 (Brooks et al., 1983; MacKerell et al., 1998), leading to an all atom representation with a total number of 7589 atoms. Subsequently, the hydrogen atom positions were relaxed by energy minimization using the CHARMM22 force field and keeping all other atoms fixed. For this optimization, all titratable groups were in their standard protonation state (acidic amino acids were deportonated, and basic amino acids were protonated), all triptophans and tyrosines were neutral, the diphosphate carried two negative charges, flavin was –1 charged, folic acid possessed a total charge of –1 (two negatively charged carboxylates and an unit positive charge on nitrogen N6).

To compute the electrostatic energies, we solved the LPBE for DNA photolyase with a three-step grid focusing procedure starting from a 162 Å cube lattice with a grid spacing of 2.0 Å, followed by a 101 Å cube with 1.0 Å grid spacing and finally a 22.75 Å cube with a grid spacing of 0.25 Å. The two lattices of lower resolution were centered with respect to the geometric center of photolyase. The lattices with highest resolution were centered at the corresponding titratable groups. The LPBE was solved using the program MULTIFLEX (Bashford & Gerwert, 1992; Bashford, 1997).

The approach to determine the protonation and redox patterns of a protein that was applied here, is exclusively based on the computation of electrostatic energies. The electrostatic energy differences of titratable groups in the protein environment were evaluated relative to suitable model compounds, which can serve as a reference. For titratable amino acids, the model compounds are the corresponding isolated amino acids in aqueous solution, where amino and carboxylate groups are neutralized and modified by the blocking groups. The experimental pK_a values of the model compounds determine the electrostatic energies of isolated titratable groups in aqueous solution, and electrostatic calculations should compute the pK_a shift of titratable groups that is caused by protein environment. As, it is already explained in Chapter 2, three additional energy terms describe these pK_a shifts. They are the Born-solvation energy, the interaction energy between titratable groups and background charges, and the energy of coupling between titatable groups in their charged states. For these computations, a dielectric constant of $\varepsilon_p = 4$ inside and $\varepsilon_s = 80$ outside of the protein was

applied. An ion exclusion layer of 2 Å and a solvent probe radius of 1.4 Å were used. The mobile ion charges in aqueous solution were modeled by an ionic strength of 100 mM. The redox potential of the solvent was set to E_{sol} = 0 mV.

Since the total number of 167 protonatable and redox-active groups in photolyase is too large, a direct evaluation of the Boltzmann averaged sum (eq. 2.48) is not possible. Therefore, we applied a Monte Carlo (MC) titration method with the Metropolis sampling criterion, for which we used the program KARLSBERG (Rabenstein, 1999; Rabenstein & Knapp, 2001). The redox potential of the FAD, tryptophans, tyrosine and the protonation probabilities of all relevant titratable groups in photolyase were determined by averaging over the populated protonation states of titratable groups. To improve the sampling efficiency of MC titration, double and triple MC moves were included in addition to standard single MC moves, if the coupling between titratable groups was stronger than 2.5 or 5.0 pK_a units, respectively. A set of MC moves, where it is attempted to change the charge state on the average at all titratable groups, is called an MC scan. For each pH value, we performed 1000 full MC scans, and after that 10000 reduced scans excluding the titratable groups, which are always protonated or deprotonated and do not change their protonation state. The standard deviation for each titratable group was smaller than 0.01 proton. For the pH dependent electron transfer in DNA photolyase, the whole pH range between 0 to 14 was investigated. The energy difference between two specific charge states of DNA photolyase was calculated with equation 2.49. If it was necessary, energy bias MC sampling was applied to reduce the statistical error of the obtained results. For more details about using bias energies see the corresponding section in Chapter 2.

7.2.2. Titratable groups

Arginine, aspartate, cysteine, glutamate, histidine, lysine, tyrosine, and C- and N-termini were considered as titratable groups. In the unprotonated state of histidine two tautomers are possible. Both were considered in our calculation (Bashford et al., 1993). Hence, we could calculate the fraction of ε– and δ–histidine tautomers. In addition, also the diphosphoric acid (DPA) as part of FAD, and the oxidized tryptophan ($WH^{\bullet+}$) and tyrosine ($YH^{\bullet+}$) were considered as titratable. MHTF involves two acidic groups. One is equivalent to the side chain of glutamate the other to the C-terminal group. We treated them as two independent titratable groups. The tryptophan triad, the nearby tyrosine Y464 and the flavin redox pair $FADH^{\bullet}/FADH^{-}$ were considered to be redox-active. Explicit water molecules were not included in computation and therefore water did not need to be considered as titratable. Anyway, their pK_a values in aqueous solution, −1.7 and 15.7, are rather extreme. We do not expect that the protein is able to stabilize H_3O^+ or OH^- ions. Although ionized water molecules may participate in transient states in proton transfer, since we deal with equilibrium states, their presence is unlikely.

The corresponding pK_a values for all titratable groups were listed in Appendix D. As reference value for tryptophan in aqueous solution, we used the redox potential of 1.07 eV (Tommos et al., 1999). For the oxidized tryptophan ($WH^{\bullet+}$), we took pK_a = 4 (Tommos et al., 1999; Solar et al., 1991). The redox potential of tyrosine was estimated to be above 1.35 eV (Tommos et al., 1999). We used 1.376 eV, derived by extrapolating experimental data. The oxidized tyrosine ($YH^{\bullet+}$) has pK_a =–2 (Tommos et al., 1999; Dixon & Murphy, 1976). FAD was divided into three parts. Two of them, DPA and flavin, were treated as two independent titratable groups. The adenine part of FAD, we considered as non-titratable. We used –290

mV (Heelis et al., 1992) for the potential of the redox pair $FADH^{\bullet}/FADH^{-}$. Thereby the protonation or deprotonation of flavin was not considered. For the DPA group of FAD no pK_a value was available. As estimate we took pK_a values from the corresponding free DPA (Stryer, 1988) where the equilibrium between the pair of protonation states $(HO_3R^{(1)}P–O–PR^{(2)}O_3H)^0$ / $(O_3R^{(1)}P–O–PR^{(2)}O_3H)^-$ and $(HO_3R^{(1)}P–O–PR^{(2)}O_3)^-$ / $(O_3R^{(1)}P–O–PR^{(2)}O_3)^{-2}$ is described by pK_a=6 and pK_a=8, respectively. There are two different states of DPA with charge –1: $(O_3R^{(1)}P–O–PR^{(2)}O_3H)^-$ and $(HO_3R^{(1)}P–O–PR^{(2)}O_3)^-$. Namely, the diphosphate (DPA) is bound on one side to adenine and on other side to flavin, but also their protein environments differ, what causes the two phosphates not to be equivalent. The program MEAD (Bashford & Karplus, 1991) available to calculate the electrostatic energies of titratable groups in different protonation states can not treat groups with more than two protonation states. To find out whether the protonation equilibrium of DPA is shifted toward the protonation states DPA^-/DPA^{-2} or toward DPA^0/DPA^-, we considered both equilibria separately and described the two different protonation states of DPA^- in the same way as we did it for histidine. For more technical details, see Chapter 2.

7.2.3. Atomic partial charges

Using an appropriate set of charges is critical to obtain reliable results for electrostatic energies. A proper choice of charges is in part a matter of experience. Most of the charges that we used in this application have been used successfully before to calculate the electrostatic energies, protonation probabilities of titratable groups and redox potentials of cofactors in proteins (Rabenstein et al., 1998a,b; Vagedes et al., 2000; Rabenstein & Knapp, 2001; Popović et al., 2001a). Additional charges that were needed for computations of electrostatic energies in this application were computed with procedures that we used in such applications before.

The atomic partial charges of the amino acids including the protonated and deprotonated states of the titratable amino acids, were taken from the CHARMM22 parameter set (MacKerell et al., 1998). The acidic hydrogen atom of protonated glutamate and aspartate is not represented explicitly. Instead, appropriate charges at the two carboxyl oxygen atoms are assigned symmetrically. A similar treatment was applied for the deprotonated form of lysine and arginine, where the calculated charges of equivalent polar hydrogens are symmetrically redistributed among them. The atomic partial charges that are not included in the CHARMM22 parameter set were calculated quantum-chemically with program SPARTAN 4.0. Using the CHELPG-like method (Breneman & Wiberg, 1990) implemented in SPARTAN, we adjusted the atomic partial charges to represent the electrostatic potential calculated from the wave functions faithfully. That was done for all titratable residues (Arg, Lys, Cys, Tyr, Trp, N- and C-terminus), where only the standard protonation state was available. More details about calculating atomic partial charges of titratable residues can be found in section 6.1.3, too. The charge distributions of FAD (including the DPA group) and MTHF (including the two acidic groups) were calculated with the Hartree-Fock method from GAUSSIAN98 (Frisch et al., 1998) using the 6-31G* basis set. The atomic partial charges were obtained from the electronic wave functions by adjusting the electrostatic potential in the neighborhood of the molecules with the Merz-Kollman approach (Besler et al., 1990). The atomic partial charges of all titratable residues, including the FAD, MTHF and the radical states of Trp and Tyr, whose charges were not used in earlier applications, are given in Appendix E, Table E1 and E3. The structural formulas of folic acid (MTHF) and flavin adenine dinucleotide ($FADH^-$) can also be found there.

7.3. Results and Discussions

7.3.1. Protonation states in photolyase

The model of radical transfer, which we want to support and complete by this computations, was recently studied by time resolved absorption spectroscopy at the pH value of 7.4 in DNA photolyase from *E. coli* (Aubert, et al., 2000). Most of the titratable groups in DNA photolyase are at pH= 7.4 in the standard protonation state, i.e. the basic residues are positively charged and the acidic residues are negatively charged. The histidines are mostly neutral, thereby the proton resides on δ- or ε-nitrogen. There are three exceptions (His44, His199 and His410), where the fraction of double protonated form is relatively large (0.87, 0.38 and 0.53, respectively). Folic acid is situated on the surface of photolyase opposite to flavin. Its two acidic groups are completely solvent exposed and therefore both are unprotonated. In aqueous solution at pH = 7, the two phosphate groups of DPA are partially and symmetrically protonated, carrying together one proton, but they are fully deprotonated in DNA photolyase. The stabilization of the two unit negative charges at the DPA group in photolyase is facilitated by orienting the polar groups of protein – the backbone NH groups and the side chain hydroxyl groups optimally. The phosphate oxygens on the adenine side form the following H-bonds: O1-Trp271(Nε) 2.94 Å, O1-Ser235(Oγ) 2.70 Å, O1-Ser235(N) 2.88 Å, O2-Tyr222(Oη) 2.70 Å; while the phosphate oxygens close to flavin form the following H-bonds: O1-Ser238(N) 3.08 Å, O1-Leu237(N) 3.19 Å, O2-Arg236(N) 2.67 Å, O2-Thr234(Oγ) 2.75 Å. As one can see there is no salt bridge interactions between the protein titratable groups and DPA group of FAD. Instead of that, the DPA oxygens are bound by the hydrogen bonds with the polar groups of the protein. Since the DPA oxygens form eight H-bonds with their protein environment, it is not so surprisingly that the DPA group carries two negative charges, when FAD is bound to the DNA photolyase. The only titratable residues in non-standard protonation state, which at the same time vary their protonation probabilities with a change in the charge states of the tryptophan triad are Glu274, Asp354, Asp374, Lys454, N-terminus and four histidines (H44,H199, H294, H453). Their protonation pattern at pH = 7.4 are listed in Table 7.1. From these residues, only Glu274 and Asp374 are not too far from FADH, but none of them is close to the tryptophan triad (Fig. 7.3). The acidic group of Glu274 is situated on the protein surface but it is not fully solvent exposed. It is partially protonated, probably due to the double negative charge of the DPA group in its neighborhood. Asp354 is the titratable residue whose protonation varies the most with a change in the charge state of the tryptophan triad. However, it is not very close to any of the three tryptophans (Fig. 7.3). Its edge-to-edge distance is 10.9 Å to W382 and 10.7 Å to W306. From 15 histidines in photolyase only four (displayed in Fig. 7.3) vary their protonation pattern with a change in the charge state of the tryptophan triad. Only one of them, His294, is close to the intermediate tryptophan W359 (6.1 Å edge-to-edge distance). The fact that none of the titratable residues couples strongly with the different charge states of the tryptophan triad takes care for a low reorganization energy of the ET processes between the tryptophan triad. The calculated total charge of photolyase and the sum of charges from the tryptophan triad and the nine residues displayed in Table 7.1 (last two columns) agree well for the different charge states of the tryptophan triad indicating that these are the most relevant residues responsible for changes of the total charge in photolyase.

The pK_a value of the positive tryptophan radical ($WH^{\bullet+}$) in aqueous solution is 4 (Tommos et al., 1999; Solar et al., 1991). Its deprotonation leads to the neutral radical state $W^{\bullet}$. Since W306 is partially solvent exposed in DNA photolyase, it behaves similar as in aqueous solution. The calculated pK_a values are 2 for W306 and –14 and –11 for the buried tryptophans W359 and W382, respectively. The pH dependence of the deprotonation energy of three tryptophan cation radicals is displayed in Fig. 7.4. The pH dependence of the

Table 7.1. Non-standard protonation probability of residues in DNA photolyase

charge state of photolyase	Glu 274	Asp 354	Asp 374	Lys 454	N-term	His44			His199			His294			His453			[a] *reduced* sum of protons	[b] *total* sum of protons
						double	δ	ε	double	δ	ε	double	δ	ε	double	δ	ε		
$FADH^-WH^{\bullet+}WH$ WH	0.385	0.626	0.016	0.701	0.277	0.807	0.003	0.189	0.339	0.239	0.422	0.004	0.555	0.441	0.045	0.772	0.182	0.196	0.23
$FADH^-WH$ $WH^{\bullet+}$ WH	0.504	0.771	0.033	0.677	0.282	0.838	0.003	0.160	0.370	0.242	0.387	0.001	0.419	0.580	0.033	0.754	0.213	0.505	0.51
$FADH^-WH$ WH $WH^{\bullet+}$	0.565	0.777	0.057	0.684	0.280	0.851	0.002	0.147	0.375	0.238	0.387	0.009	0.663	0.328	0.030	0.762	0.208	0.624	0.66
$FADH^-WH$ WH $W^{\bullet}$	0.595	0.894	0.059	0.676	0.271	0.861	0.002	0.137	0.373	0.240	0.387	0.014	0.692	0.294	0.022	0.764	0.213	-0.239	-0.22
$FADH^-WH$ $W^{\bullet}$ WH	0.586	0.916	0.062	0.678	0.273	0.849	0.002	0.149	0.368	0.252	0.380	0.012	0.660	0.328	0.015	0.771	0.215	-0.245	-0.20
$FADH^-W^{\bullet}$ WH WH	0.617	0.908	0.063	0.678	0.275	0.969	0.002	0.129	0.382	0.242	0.376	0.012	0.688	0.300	0.018	0.768	0.215	-0.082	-0.16
$FADH^{\bullet}WH$ WH WH	0.221	0.869	0.000	0.679	0.275	0.671	0.004	0.325	0.258	0.260	0.482	0.009	0.645	0.346	0.022	0.762	0.216	0.000	0.00

With the exception of histidines, we listed all titratable residues of photolyase, which deviate by at least 0.05 unit charges from the standard protonation state at pH=7.4. From the 15 histidines we listed only those four whose protonation probabilities vary by more than 0.05. The small deviations between the total sum and the reduced sum of protons demonstrates that the main contribution to changes in the total charge of photolyase is due to these nine residues.

[a] Sum of protonation probabilities of the nine listed titratable groups including the protons in the tryptophan triad relative to the sum of the ground state $FADH^{\bullet}$ WH WH WH probabilities, which is $\sum p_0 = 3.004$.

[b] Sum of all protons in photolyase relative to the sum of protons in the ground state $FADH^{\bullet}$ WH WH WH.

deprotonation energy is approximately linear for $WH^{\bullet+}306$ and close to the behavior of a fictitious non-interacting tryptophanyl cation radical in aqueous solution (dashed line in Fig. 7.4). The deprotonation energy of $WH^{\bullet+}382$ and $WH^{\bullet+}359$ is considerably higher than of the solvent exposed $WH^{\bullet+}306$. Hence, the two other tryptophans prefer even more than W306 to be in the neutral radical state $W^{\bullet}$. This behavior is expectable, since bare charges can be accommodated easier in a high dielectric medium than in the protein environment of low dielectric constant. Additionally, one can also see, that the reprotonation energy of $W306^{\bullet}$ is at pH 5.4 twice lower than at pH 7.4, what can explain the acceleration of the charge recombination (back reaction) with decreasing the pH.

The deprotonation of different tryptophan cation radicals causes the differences in the total charge of the protein. The formal total charge of the DNA photolyase is computed by using the standard protonation state of all titratable residues and assuming that the histidines are neutral. Considering that folic acid possesses a total charge of –1 (two negatively charged carboxylates and a unit positive charge on N6) and FAD a total charge of –3 (due to DPA and flavin) the formal total charge of photolyase is –6 in the resting state $FADH^{\bullet}$-WH-WH-WH-YH and in the four possible charge separated states $FADH^{-}$-$WH^{\bullet+}$-WH-WH-YH, $FADH^{-}$-WH-$WH^{\bullet+}$-WH-YH, $FADH^{-}$-WH-WH-$WH^{\bullet+}$-YH, and $FADH^{-}$-WH-WH-WH-$YH^{\bullet+}$ (Fig. 7.6). Consequently, the formal total charge is –7 if one of the tryptophans from the triad or the tyrosine becomes deprotonated. The total charge of photolyase computed from the distribution of protonation pattern is close to –5 if all tryptophans from the triad and the tyrosine Y464 are protonated. The calculated total charge diminishes by a fraction of a unit charge, if one of the buried tryptophans or the tyrosine becomes deprotonated (W382: -0.39; W359: -0.71; Y464: -0.54), whereas it decreases by almost a unit charge (-0.88) if the solvent accessible W306 is deprotonated (see Fig. 7.6). Hence, the protein tries in part to compensate for the decrease in charge if a buried tryptophan becomes deprotonated by an increase in protonation at a number of other residues. This is expectable, since the photolyase is already negatively charged (≈ -5), and deprotonation of a buried tryptophan cation radical would further decrease the negative charge of the protein. However, it seems that this charge compensation is not necessary for the solvent exposed tryptophan W306.

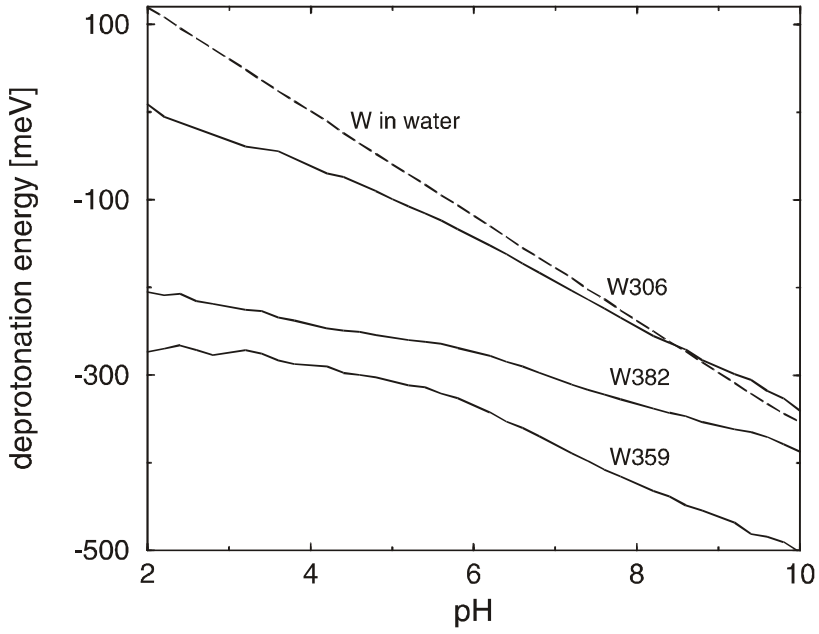

Figure 7.4: pH dependence of deprotonation free energy of the tryptophan cation radicals evaluated by calculating the electrostatic energies solving the LPBE. The dashed line refers to the pH dependence in aqueous solution. Flavin was in the reduced state $FADH^{-}$, as it corresponds to the activated photolyase.

7.3.2. Redox potentials of tryptophan triad

Oxidized tyrosine $YH^{\bullet+}$ and tryptophan $WH^{\bullet+}$ prefer to be deprotonated, since they possess pK_a values of –2 and 4, respectively (Tommos et al., 1999; Solar et al., 1991). Already in a very acidic pH range in aqueous solution, the oxidation of tyrosine or tryptophan is coupled to the deprotonation reaction, what complicates the interpretation of measurements on the redox potential. We simulated this pH dependence of the tryptophan redox potential in aqueous solution considering the three possible states, $WH^{\bullet+}$, WH, and $W^{\bullet}$ involved in the redox reaction by using a technique analog as one employed for histidine (see Chapter 2). The same was done for tyrosine (see Fig. 7.5A). We used 1.07 eV for the redox potential of tryptophan and 1.376 eV for tyrosine, which are the pH independent values at very low pH (Tommos et al., 1999; DeFelippis et al., 1991), since in this pH range a deprotonation of $WH^{\bullet+}$ ($YH^{\bullet+}$) is not possible. To avoid artifacts from the bare charges the N- and C-terminus of tryptophan (tyrosine) was methylated and amidated, respectively. The obtained pH dependences (Figure 7.5A) agree within ±10 meV with the experimental measurements (Tommos et al., 1999; Dixon & Murphy, 1976).

At very low pH, the redox potential of the redox pair $YH^{\bullet+}$/YH is about 0.3 eV higher than for the redox pair $WH^{\bullet+}$/WH in aqueous solution. It means that under this condition $YH^{\bullet+}$ can oxidize WH shifting the equilibrium of the reaction $YH^{\bullet+} + WH \rightleftarrows YH + WH^{\bullet+}$ to the right side. At neutral or higher pH, the redox potentials become more similar differing by about 60 mV but now the redox potential of the tryptophan is higher, since the oxidation goes along with the deprotonation of cationic radicals, where the pK_a value of $YH^{\bullet+}$ is –2 and of $WH^{\bullet+}$ is 4. Hence, in order to oxidize the YH, the potential of the redox pair $WH^{\bullet+}$/WH has to be more positive. As one can see from Fig. 7.6, for photolyase from *E. coli* at pH= 7.4, the considered equilibrium $YH^{\bullet+} + WH \rightleftarrows YH + WH^{\bullet+}$ is very much shifted toward the right, since the potential of the redox pair $YH^{\bullet+}$464/YH464 is 750 mV higher than of the $WH^{\bullet+}$306/WH306 pair. The reason is that Y464 is buried in the low dielectric medium of hydrophobic residues stabilizing the reduced state of YH464, while W306 is water exposed and in the neighborhood of two negatively charged aspartates (D302 and D358) stabilizing the oxidized state of $WH^{\bullet+}$306.

Figure 7.5B. exhibits the pH dependence of the redox potential of the tryptophans W306, W359 and W382, in photolyase for the redox pairs $WH^{\bullet+}$/WH (three uper dashed curves), as well as for the redox pairs WH/$W^{\bullet}$ (dashed line – W306, dotted line – W359, dashed-dotted line – W382, in the lower part of figure). The upper curves correspond to the situation, where electron transfer occurs only between the tryptophans from the triad. The three other pH dependences correspond to a simultaneous deprotonation of the $WH^{\bullet+}$ cation radical with an increase of pH. Since in the later case, the electron transfer is coupled with a deprotonation of tryptophan, the redox pairs WH/$W^{\bullet}$ show much stronger pH dependence than the corresponding redox pairs $WH^{\bullet+}$/WH. But the redox potential of the $WH^{\bullet+}$/WH pair is also pH dependent, because the deprotonation of nearby titratable groups has an influence on that. Namely, the increase of the pH will deprotonate adjacent titatable groups much more, making the total protein charge more negative, what can lead to a simultaneous oxidation of a redox-active group, decreasing its redox potential.

The coupling of the ET with changes of protonation pattern of nearby titratable groups is screened most efficiently for the solvent exposed tryptophan W306, such that the redox potential of the $WH^{\bullet+}$/WH couple exhibits very mild pH dependence (dashed lines in upper part of Fig. 7.5B). While the two other tryptophans, that well buried in interior of the protein, are more influenced by the changes of the protonation pattern and show a somewhat stronger

A

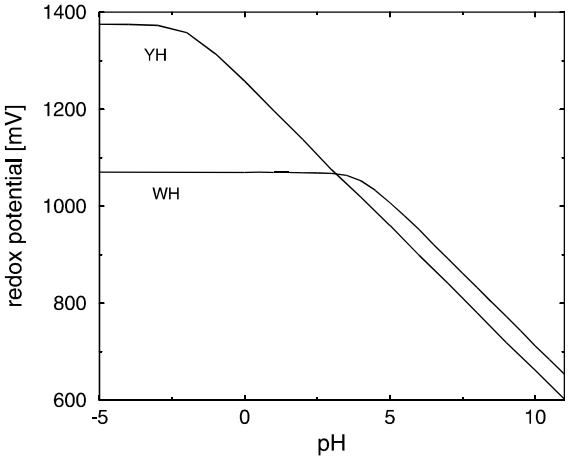

Figure 7.5: (A) The simulated pH dependences of tyrosine and tryptophan in aqueous solution. **(B)** pH dependence of the redox potentials of tryptophans from the triad in photolyase and in water. Upper curves (dashed lines): pH dependence of the redox potential of the three tryptophans from the triad remaining in the protonated state, i.e. considering the redox pair $WH/WH^{\bullet+}$. Solid line: pH dependence of tryptophan in water calculated by using a dielectric medium of $\varepsilon = 80$ and allowing the tryptophan to deprotonate at high pH as it occurs in aqueous solution. The three curves parallel to the solid line exhibit the pH dependence of the redox potential of the tryptophans from the triad in photolyase by allowing them to deprotonate in the oxidized state. Dashed line: W306; dotted line: W359; dashed-dotted line: W382.

B

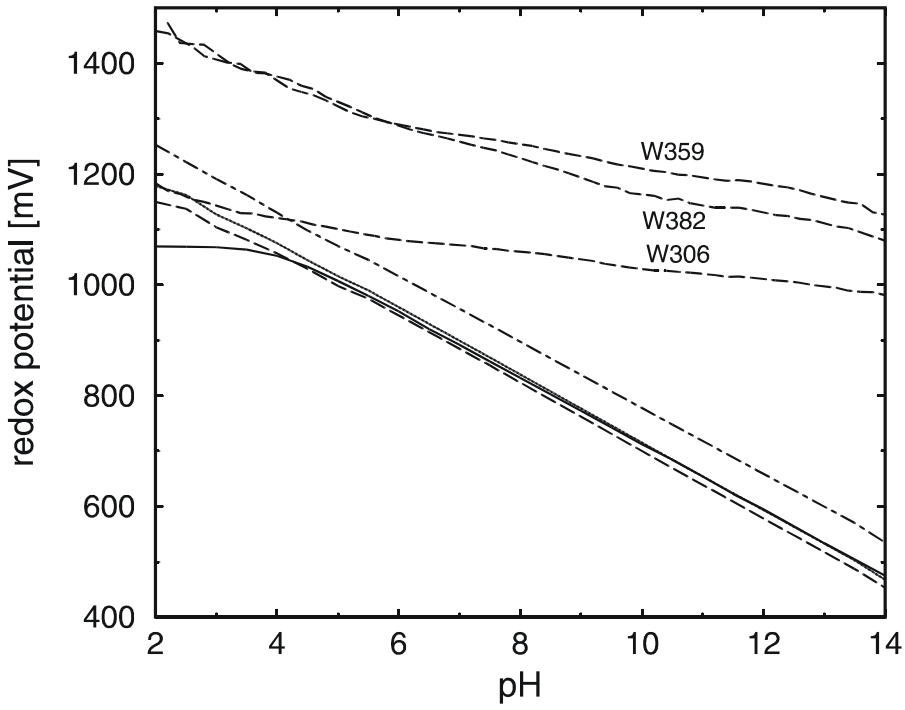

pH dependence. Thereby, their redox potentials are almost the same until pH 6.5. Considering the redox pairs $WH/W^{\bullet}$ involved in a coupled electron-proton transfer, the pH dependence of the redox potential for the tryptophans in photolyase is very similar to the one of tryptophan in aqueous solution (Fig. 7.5B). That is particularly the case for W306 and W359, which are water accessible. The redox potential of the $WH382/W^{\bullet}382$ couple has about 70 mV higher value, nevertheless its pH dependence is similar to the two others in the pH range between 4 to 14. At low pH values the redox potentials of the redox pair $WH^{\bullet+}/WH$ and $WH/W^{\bullet}$ merge, since a deprotonation of tryptophan is not any more possible. This merging occurs already at pH = 2 for the solvent exposed tryptophan W306, but occurs at lower pH for the buried tryptophans whose pK_a values are shifted to smaller values. Considering the redox pair $WH^{\bullet+}/WH$, the order of the redox potentials at pH= 7.4 is the following: W359 > W382 > W306. Probably the positive charge on $WH^{\bullet+}382$ (oxidized form) and the negative charge of flavin stabilize each other, while such stabilization disappears when the radical state is transferred to W359. As a consequence, the redox potential of the $WH^{\bullet+}382/WH382$ pair is a

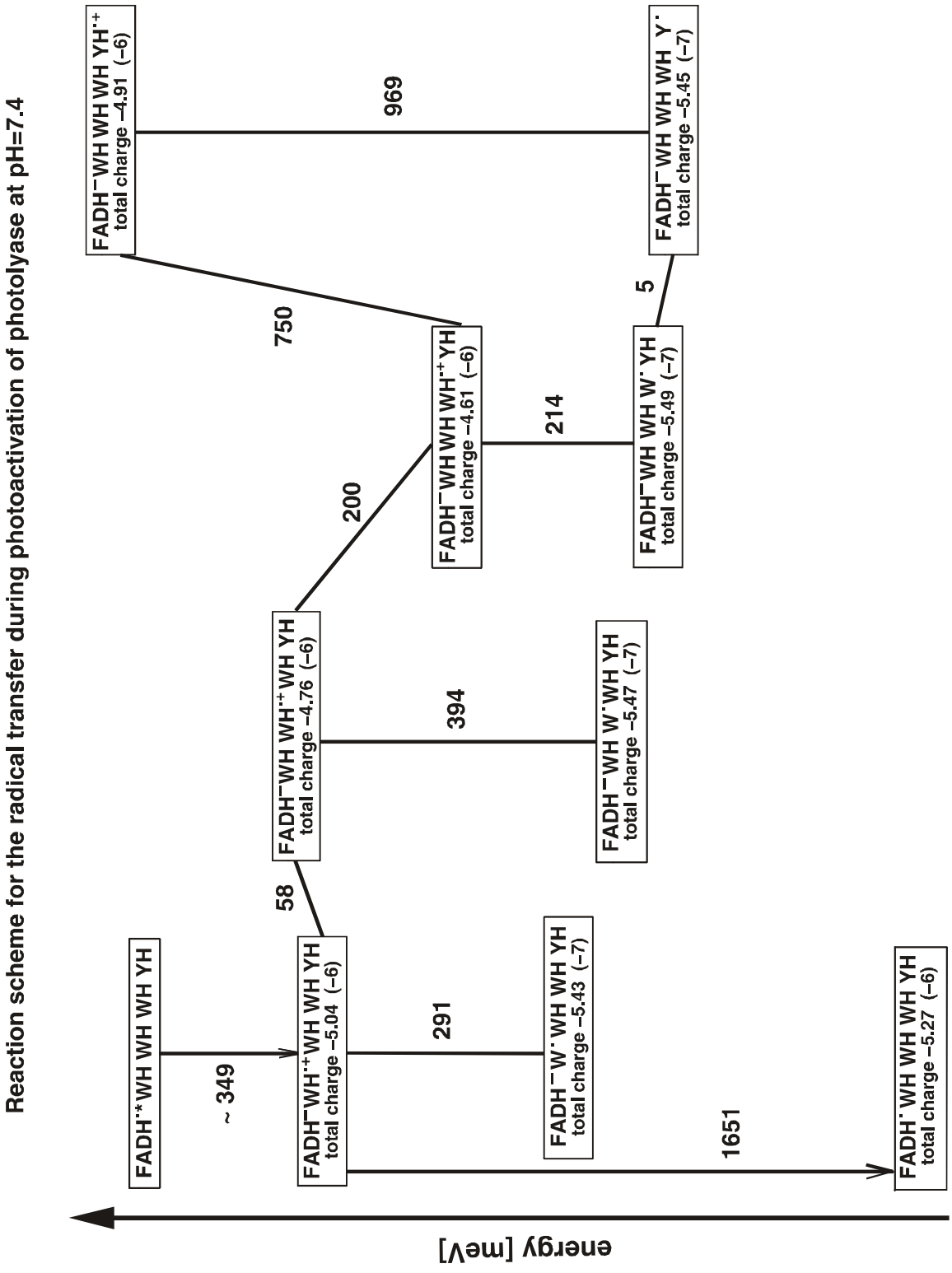

Figure 7.6: The energy scheme of the charge separation and radical transfer process in DNA photolyase of *E. coli*. Vertical solid lines connecting different states indicate changes of electronic state or protonation. More horizontal solid lines indicate ET processes. The numbers at these lines provide the difference in electrostatic energies in units of meV between the pairs of states connected by the line.

bit lower than for the $WH^{\bullet+}359$/WH359 pair. The order of the redox potentials for the redox pairs $WH/W^{\bullet}$ is as follows: W382>W359>W306, as we expect on the basis of the respective local protein environment. Namely, W382 is situated in a more hydrophobic environment than the two other tryptophans. Consequently, its redox potential is the highest. Since only W306 is directly solvent exposed, it can easily deprotonate, so its redox potential should be the lowest. The differences in the redox potentials of the $WH^{\bullet+}$/WH redox pairs correspond to the reaction energies of ET between positively charged radical states (two transitions in scheme 7.6 upper part). While the differences in the redox potentials of the $WH/W^{\bullet}$ pairs determine the energetics between three neutral (deprotonated) radical states (two transitions in scheme 7.6, lower part).

To calculate the energy difference between the ground (resting) state $FADH^{\bullet}$ WH382 and the initial charge separated state $FADH^{-}$ $WH^{\bullet+}382$, we allowed FAD to be titratable with respect to the redox equilibrium $FADH^{\bullet} \rightleftarrows FADH^{-}$, using for the model compound the redox potential of flavin in aqueous solution (–290 mV; Heelis et al., 1992). The calculated redox potential that the $FADH^{\bullet}/FADH^{-}$ pair assumes in photolyase at pH= 7.4 is –460 mV. It means that low dielectric environment of the protein stabilizes the neutral oxidized state of $FADH^{\bullet}$ even more, what can explain the fact that the resting state of photolyase contains the $FADH^{\bullet}$ form. At the same time the potential of redox pair WH382/ $WH^{\bullet+}382$ is +1191 mV. It yields the energy difference between the ground and charge separated state of 1.651 eV. In agreement with experiments we did not consider a change of the protonation state of flavin. However we obtained that its redox potential is pH dependent decreasing by 56 mV/pH, due to the deprotonation of adjacent titratable groups. In agreement with an experimental estimate (Heelis et al., 1992), the redox potential of FAD in photolyase decreases from –320 to –545 mV in the pH range from 5 to 9. Since the potential of the redox pair WH382/ $WH^{\bullet+}382$ also decreases with pH (about 35 mV/pH), the energy difference between the resting and catalytically active states of photolyase is practically not sensitive on the pH changes.

7.3.3. Energetics and reaction rates of the photoactivation process

The reaction profile of the charge separation and radical transfer process in DNA photolyase of *E. coli* is displayed in Fig. 7.6. The electronic excited state in photolyase $FADH^{\bullet *}$ is estimated to be 2 eV above the ground state $FADH^{\bullet}$ (Aubert et al., 2000). The initial charge separated state $FADH^{-}$ $WH^{\bullet+}382$ is calculated to be 1.651 eV above the ground state. Hence, there are 0.349 eV available for the charge separation process, where the nearby WH382 transfers an electron to the $FADH^{\bullet *}$. In the next step, an electron is transferred from the intermediate tryptophan W359 to the proximal W382 with a slightly positive reaction energy of +58 meV. The ET from the distal tryptophan W306 to W359 is calculated to be downhill in energy with –200 meV, favoring the radical localization on W306 already, before its deprotonation. Finally, the deprotonation of the distal tryptophan occurs at pH=7.4 with a reaction energy of –214 meV what is in agreement with an estimate that assumes W306 to behave as in solution (Aubert et al., 2000). Since this tryptophan is solvent exposed, the proton can directly be dumped into the solvent.

The two buried tryptophans may also become deprotonated, although there is no direct pathway for the proton from $WH^{\bullet+}382$ to reach the solvent and data on the W306F mutant (Li et al., 1991) do not give any indication for a deprotonation of the $WH^{\bullet+}359$ cation radical. However, a deprotonation of two buried tryptophans is energetically extremely favorable but it will be very slow as compared to the ET, which is faster than 10 ns. Even a deprotonation of the solvent exposed $WH^{\bullet+}306$ (300 ns) is almost two orders of magnitude slower than the competing ET process.

Calculating the energetics of the deprotonated radical states of the tryptophan triad, we found that the energy difference between WH359–W$^{\bullet}$306 and W$^{\bullet}$359–WH306 states is 20 meV and between WH382–W$^{\bullet}$359 and W$^{\bullet}$382–WH359 states is 45 meV (see Fig. 7.6). So, one can speculate that deprotonated radical states may possibly participate in the charge recombination (back reaction), specially if one considers that the corresponding edge-to-edge distances between the tryptophans are only 3.9 Å and 5.2 Å, and the hydrogen transfer may be supported by two crystal waters (H_2O613 and H_2O841) and Asp358. But such a transfer, where the neutral radical state moves from W306 via W359 to W382, should assume a hydrogen atom transfer or a coupled proton–electron transfer, what may energetically be possible, but is kinetically probably very slow.

According to the Marcus theory (Marcus & Sutin, 1985), the electron transfer rate depends on the reaction free energy. To estimate the rate for the exergonic ET reactions in the *E. coli* photolyase, we used the empirical expression (Page et al., 1999):

$$\log_{10}\left(k^{ET}_{exergonic}\right) = 13.0 - 0.6(D - 3.6) - 3.1(\Delta G + \lambda)^2 / \lambda \qquad (7.1)$$

where ΔG is the free energy difference of exergonic ET reaction, D is the closest distance between two reactants (electron donor and acceptor) and λ is the reorganization energy governing the ET process. For the reorganization energy of the ET processes, we used the generic value of 1 eV (Page et al., 1999). Equation 7.2 estimates the rate of the endergonic step by using equation 7.1 for the opposite exergonic step and dividing it by the temperature-dependent Boltzmann factor, or equilibrium constant ($10^{\Delta G/0.06}$ at T=300K).

$$\log_{10}\left(k^{ET}_{endergonic}\right) = 13.0 - 0.6(D - 3.6) - 3.1(-\Delta G + \lambda)^2 / \lambda - \Delta G / 0.06 \qquad (7.2)$$

Here ΔG is the free energy difference of endergonic ET reaction, which has opposite sign from the corresponding free energy of the exergonic step.
The ET of the forward reaction was measured to be faster than 10 ns (Aubert et al., 2000). The overall rate of the forward ET process is dominated by the weakly endergonic ET step from W359 to W382. Using the ΔG= 0.058eV, D= 5.2 Å for edge-to-edge distance between the tryptophans, and the generic value λ= 1.0 eV in eq. 7.2, we obtained the estimated rate value $k^{ET}_{forward} = 2.1*10^8 s^{-1}$. This value of the rate constant of the forward ET process is consistent with the fact that the tryptophanyl radical WH$^{\bullet+}$306 appears in less than 10 ns. Similarly, the rate of the exergonic ET step form W306 to W359 is estimated to be $6.9*10^{10}$ s^{-1}, using the parameters: ΔG= –0.2 eV, λ= 1.0 eV, D= 3.9 Å, in eq. 7.1. The reverse ET process leading to charge recombination is dominated by the endergonic ET step: WH359–WH$^{\bullet+}$306 $\rightarrow$ WH$^{\bullet+}$359–WH306. On the basis of eq. 7.2, its rate is estimated to be $3.2*10^6$ s^{-1}. Hence, the cationic tryptophan radical is most of the time localized at W306, what facilitates deprotonation of W306 stabilizing the catalytically active charge state FADH$^-$ in photolyase.

The deprotonation rate of WH$^{\bullet+}$306 at pH= 7.4 was measured to be $k^{PT}_{forward} = 3.3x10^6$ s^{-1}, assuming direct proton transfer from WH$^{\bullet+}$ to H_2O molecules of solvent (Aubert et al., 2000). If the reprotonation reaction of W$^{\bullet}$306 is governed by the same activation energy the corresponding rate can be estimated using the formula:

$$k^{PT}_{back} = 3.3x10^6 \ s^{-1} * \exp(-0.214eV/k_BT) = 840 \ s^{-1} \qquad (7.3)$$

The back reaction is kinetically slowed down, in comparison to the forward reaction of deprotonation, since the proton from the partially solvent exposed W306 can easily be dumped in the solvent but may not be so readily available for reprotonation. Comparing the reaction rates, it is obvious that the electron back transfer is much faster (four orders of

magnitude) than the reprotonation of $W^{\bullet}306$, such that the overall rate of charge recombination is dominated by the proton uptake: $W^{\bullet}306 + H^{+} \rightarrow WH^{\bullet+}306$. This is also supported by experimental results, which show a strong acceleration of the back transfer at lower pH values (Aubert et al. 2000). The calculated rate of proton uptake k_{back}^{PT} =840 s^{-1} at pH= 7.4 corresponds to a lifetime of 1.2 ms for the neutral radical state $FADH^{-}$ WH WH $W^{\bullet}$, that correlates within an order of magnitude with the measured lifetime of 17 ms (Aubert et al. 2000).

In photolyase from *A. nidulans* the radical state resides finally at about 40% on a tyrosine (Aubert et al., 1999a, 1999b). In photolyase from *E. coli*, the closest and only available tyrosine for the ET, 3.6 Å away from the tryptophan W306, is Y464. However, experimentally such an ET is not observed. To clarify the question why photolyase from *E. coli* behaves different in that respect, we computed the energetics of a possible radical transfer from W306 to Y464. The corresponding ET from YH464 to $WH^{\bullet+}306$ is strongly endergonic by 750 meV, since Y464 is buried in the low dielectric medium of the protein. For the same reason the deprotonation is strongly exergonic by 969 meV, such that the neutral radical states $W^{\bullet}306$–YH and WH306–$Y^{\bullet}$ are nearly isoenergetic (5 meV difference). We also noticed, that the energy level of the positive radical state $YH^{\bullet+}464$ is even 251 meV higher than the energy level of the UV-light excited state ($FADH^{\bullet*}$). Using eq. (7.2) with a reorganization energy of λ = 1.0 eV and distance D= 3.6 Å, the endergonic ET rate is estimated to be only 2 s^{-1}. That is more than one order of magnitude smaller than overall rate of charge recombination. Moreover, the lifetime of the $YH^{\bullet+}464$ state, limited by electron back transfer from WH306 to about 10^{-13} s, is extremely short. Beside that, this tyrosine is buried in a hydrophobic environment where a potential proton acceptor is missing, what excludes the possibility of deprotonation of the $YH^{\bullet+}464$ cation radical. Since the rings of the Y464 and W306, with their polar hydrogen atoms are oriented to point away from each other (see Fig. 7.3) and without obvious pathway between them, also a direct hydrogen transfer is probably very slow in comparison with the competing charge recombination process. It seems that on this short time scale only a back electron transfer is likely to occur. Y464 is buried in the low dielectric medium of the protein and it is not water exposed, what raises the difficulties of its deprotonation. In photolyase from *A. nidulans* the corresponding tyrosine Y468 is solvent exposed. Accordingly, we expect that the cationic radical state $YH^{\bullet+}468$ from *A. nidulans* has a much lower energy than has $YH^{\bullet+}464$ state from *E. coli*, such that the neutral radical state of Y468 can be reached.

Very recently, the electrostatic calculations have been performed for DNA photolyase from *A. nidulans* (Winkelmann et al., unpublished results), using the same approach and with the same set of charges as for the calculations on *E. coli* (Popović et al., 2001b). The possible radical transfer chain (FAD-W390-W367-W314-Y468) of *A. nidulans* DNA photolyase was investigated, which is analog to the radical chain of *E. coli* photolyase. However, Y468 is 8.6Å away from the last of three tryptophans in the chain, W314. Nevertheless, it is the closest tyrosine, since the next one is more than 14Å away. The electrostatic energy profile for the radical transfer during the photoactivation was calculated at pH= 7.0. The results show that the electrostatic energy only goes downhill through the radical transfer chain of the tryptophans. The ET from the intermediate tryptophan W367 to proximal W390 is –53 meV, while the ET from the distal tryptophan W314 to W367 is calculated to be even more downhill in energy with –188 meV. That would very easy stabilize the radical state on W314. Since, the relatively small energy (+176 meV) is needed for further transfer of radical character to Y468, such transfer is possible, as was also shown by experimental data (Aubert et al., 1999a). In contrast to *E. coli*, where Y464 is inside the protein, Y468 in *A. nidulans* is partially solvent accessible what may facilitate such an ET process and the subsequent deprotonation of $YH^{\bullet+}468$. This deprotonation is strongly exergonic by –869 meV, and the

neutral radical state WH314–$Y^{\bullet}$468 is by 361 meV more stable than $W^{\bullet}$314–YH468. All these data qualitatively agree with the experimental findings from Brettel and cooworkers, that 40% of radical state, in *A. nidulans*, resides on Y468, while 60% of radical state probably remain on W314 either in protonated ($WH^{\bullet+}$314) or even more likely in deprotonated form ($WH^{\bullet}$314). The deprotonation of the partially solvent accessible tryptophan W314 is calculated to be very favorable with energy of –332 meV, at pH=7.0. Anyhow, the spectral data show that only 40% of the tryptophanyl radicals were reduced by tyrosine, while the remaining tryptophanyl radicals were reduced finally through a back-reaction with $FADH^{-}$ (Aubert et al., 1999a). However, these are only preliminary results, since the exact pathway in DNA photolyase from *A. nidulans* is still experimentally not known. Inspection of the X-ray structure shows that there are other nearby tryptophans and tyrosines which could take part in the radical transfer process of photoactivation. Therefore, several other possible radical transfer chains must also to be examined.

7.4. Conclusion

Our results are consistent with all experimental data and findings (Aubert, et al., 2000) and provide further insight in the photoactivation process of DNA photolyase from *E. coli*. The energies of all relevant states and the calculated rates for the most relevant processes agree well. The more detailed description of the charge separation and radical transfer from these computations yields the following conclusions.

To form the initial charge separated state $FADH^{-}$ from the electronic exited state FADH* a sufficient amount of energy (349 meV) is available. While the first ET from W359 to W382 is slightly uphill (+58 meV), the ET from W306 to W359 is downhill in energy by 200 meV already stabilizing the radical state at the distal tryptophan W306. A further stabilization in energy by 214 meV, occurs by the deprotonation of the radical state $WH^{\bullet+}$306, leading to the neutral radical $W^{\bullet}$306. We used the generic value of 1 eV (Page et al., 1999) for the reorganization energy of the ET processes in proteins. The energy of the cationic radical state of $WH^{\bullet+}$306 is lower than the one of W382 and W359, presumably since W306 is solvent exposed and can therefore better accommodate its positive charge, while the neutral radical state of the tryptophans differ by no more than 65 meV. The charge recombination process, yielding back the enzyme in the resting state with $FADH^{\bullet}$, is dominated by reprotonation of $WH^{\bullet+}$306. The calculated lifetime of 1.2 ms correlates well with the measured lifetime of 17 ms (Aubert, et al., 2000). In contrast to photolyase from *Anacystis nidulans* the radical state is not transferred to a tyrosine. Although there is a tyrosine, Y464, close to the distal W306 from the triad. Presumably, the electron transfer from the tyrosine Y464 to W306 is too endergonic and a direct hydrogen transfer is too slow. The coupling of specific charge states of the tryptophan triad with protonation pattern of titratable residues is small.

The results on the photoactivation of DNA photolyase from *E. coli* may be relevant for the other photolyases (class I and class II) and also for the cryptochrome blue-light receptors in plants and animals, which are flavoproteins similar in sequence to photolyases (Cashmore et al., 1999). Inspecting the aligned amino-acid sequences of photolyases and cryptochromes, it was noticed that the tryptophan residues W382, W359 and W306 are uniformly conserved (Kanai et al., 1997). This observation may suggest that the electron transfer chain described here could be involved in the function of all photolyases, and of blue light receptors as well. Of course, some structural specifics, as for instance, the solvent accessibility of these tryptophans or the presence of possible tyrosines on the protein surface could also play a significant role in determining the photoactivation process and radical pathway in these proteins.